ARTICLE OPEN

Check for updates

Maternal depressive symptoms, neonatal white matter, and toddler social-emotional development

Alexandra Lautarescu[1,2,11]✉, Alexandra F. Bonthrone[1,11], Maximilian Pietsch[1,2], Dafnis Batalle[1,2], Lucilio Cordero-Grande[1,3,4], J-Donald Tournier[1], Daan Christiaens[1,5], Joseph V. Hajnal[1], Andrew Chew[1], Shona Falconer[1], Chiara Nosarti[1,6], Suresh Victor[1,7], Michael C. Craig[2,8], A. David Edwards[1,7,9,10] and Serena J. Counsell[1]

Maternal prenatal depression is associated with increased likelihood of neurodevelopmental and psychiatric conditions in offspring. The relationship between maternal depression and offspring outcome may be mediated by in-utero changes in brain development. Recent advances in magnetic resonance imaging (MRI) have enabled in vivo investigations of neonatal brains, minimising the effect of postnatal influences. The aim of this study was to examine associations between maternal prenatal depressive symptoms, infant white matter, and toddler behaviour. 413 mother-infant dyads enrolled in the developing Human Connectome Project. Mothers completed the Edinburgh Postnatal Depression Scale (median = 5, range = 0–28, $n = 52$ scores ≥ 11). Infants ($n = 223$ male) (median gestational age at birth = 40 weeks, range 32.14–42.29) underwent MRI (median postmenstrual age at scan = 41.29 weeks, range 36.57–44.71). Fixel-based fibre metrics (mean fibre density, fibre cross-section, and fibre density modulated by cross-section) were calculated from diffusion imaging data in the left and right uncinate fasciculi and cingulum bundle. For $n = 311$, internalising and externalising behaviour, and social-emotional abilities were reported at a median corrected age of 18 months (range 17–24). Statistical analysis used multiple linear regression and mediation analysis with bootstrapping. Maternal depressive symptoms were positively associated with infant fibre density in the left (B = 0.0005, $p = 0.003$, $q = 0.027$) and right (B = 0.0006, $p = 0.003$, $q = 0.027$) uncinate fasciculus, with left uncinate fasciculus fibre density, in turn, positively associated with social-emotional abilities in toddlerhood (B = 105.70, $p = 0.0007$, $q = 0.004$). In a mediation analysis, higher maternal depressive symptoms predicted toddler social-emotional difficulties (B = 0.342, t(307) = 3.003, $p = 0.003$), but this relationship was not mediated by fibre density in the left uncinate fasciculus (Sobel test $p = 0.143$, bootstrapped indirect effect = 0.035, SE = 0.02, 95% CI: [−0.01, 0.08]). There was no evidence of an association between maternal depressive and cingulum fibre properties. These findings suggest that maternal perinatal depressive symptoms are associated with neonatal uncinate fasciculi microstructure, but not fibre bundle size, and toddler behaviour.

Translational Psychiatry (2022)12:323 ; https://doi.org/10.1038/s41398-022-02073-y

INTRODUCTION

Maternal depression is one of the most common prenatal complications and is related to poor neurodevelopmental and psychiatric outcomes in offspring [1]. These outcomes may be explained, at least in part, by changes in the developing brain during intrauterine life [2, 3]. However, most research is based on older participants, making it difficult to separate the effects of prenatal and postnatal environment.

Recent advances in magnetic resonance imaging (MRI) have enabled in vivo investigations of neonatal brains [4]. A growing number of diffusion MRI studies suggest that maternal depression and anxiety are associated with changes in the infant brain, with reports of lower Fractional Anisotropy (FA) [5–7] and higher FA [8, 9] in widespread regions. Previous literature suggests that frontal-limbic areas including the uncinate fasciculus and the cingulum may be particularly vulnerable to the effects of maternal stress [10–15].

Changes in the micro- and macrostructure of these tracts have also been linked to the development of mood disorders, social information processing, and behavioural and social development [16–20]. Neonatal microstructure of the right anterior cingulum bundle is associated with increased internalising symptoms, inattention and impaired social cognition at age 5 in children born prematurely [21]. Altered white matter microstructure [22],

[1]Centre for the Developing Brain, Department of Perinatal Imaging and Health, School of Biomedical Engineering and Imaging Sciences, King's College London, St Thomas' Hospital, London, UK. [2]Department of Forensic and Neurodevelopmental Sciences, Institute of Psychiatry, Psychology and Neuroscience, King's College London, London, UK. [3]CIBER de Bioingeniería, Biomateriales y Nanomedicina, Instituto de Salud Carlos III, Madrid, Spain. [4]Biomedical Image Technologies, ETSI Telecomunicación, Universidad Politécnica de Madrid, Madrid, Spain. [5]Department of Electrical Engineering, ESAT/PSI, KU Leuven, Leuven, Belgium. [6]Department of Child and Adolescent Psychiatry, Institute of Psychiatry, Psychology and Neuroscience, King's College London, London, UK. [7]Neonatal Unit, Evelina London Children's Hospital, London, UK. [8]National Female Hormone Clinic, South London and Maudsley National Health Service Foundation Trust, London, UK. [9]MRC Centre for Neurodevelopmental Disorders, King's College London, London, UK. [10]EPSRC/Wellcome Centre for Medical Engineering, King's College London, London, UK. [11]These authors contributed equally: Alexandra Lautarescu, Alexandra F. Bonthrone. ✉email: Alexandra.Lautarescu@kcl.ac.uk

Received: 2 May 2022 Revised: 1 July 2022 Accepted: 18 July 2022
Published online: 09 August 2022

particularly in the uncinate fasciculus, has been linked with social difficulties in young autistic children [19], and emotional development in children born very preterm [23]. Altered white matter development in the neonatal period may be an antecedent for social communication or behavioural difficulties in early childhood.

It is important to note that outcomes in offspring exposed prenatally to poor maternal psychological wellbeing are characterised by a large degree of heterogeneity, and not all children have poor outcomes [1, 2]. There is also evidence that male and female offspring may be affected differently [24]. Similarly, adverse outcomes and altered brain structure and function are not just associated with maternal clinical depression, but also with subthreshold depressive symptoms [2, 3], emphasising the importance of using a dimensional approach.

It is possible that individual differences in developmental outcomes in at risk infants are in part explained by differences in early brain development. Therefore, it is necessary to understand whether the association between maternal depressive symptoms and behavioural outcomes is mediated by early brain development. Prior mediation and moderation studies have mainly focused on biological indicators of stress [25, 26], with only a few studies investigating self-reported psychological wellbeing [27, 28]. Moog and colleagues [28] reported that variations in hippocampal volume may mediate the association between maternal perceived stress and infant social-emotional function.

The diffusion MRI literature linking maternal self-reported depressive symptoms with offspring brain development and behaviour is scarce. Hay and colleagues [13] reported that amygdala-prefrontal structural connectivity mediated the association between prenatal depression and externalising behaviour in males. However, imaging in this study was performed at 4 years of age, making it difficult to separate the effects of the prenatal and postnatal environment. To our knowledge, there has been only one such study in a smaller neonatal sample ($n = 80$, [15]) which reported that, while there was no direct association between maternal depressive symptoms and white matter properties, whole-brain FA moderated the association between maternal depression and negative reactivity.

It is important to note that the majority of these studies are based on the diffusion tensor model [29] which is limited by its inability to describe more than one dominant fibre orientation and to provide accurate information in voxels that contain crossing and kissing fibres [30]. However, crossing fibres exist in over 90% of white matter voxels in the adult brain [31]. In addition, DTI metrics may be affected by multiple features of the underlying microstructure.

Modern data acquisition techniques such as those employed as part of the developing Human Connectome Project (dHCP, developingconnectome.org) allow more information to be extracted from the diffusion-weighted signal. Fixel-based analysis (FBA, [32]) achieves microstructural and spatial specificity and characterises multiple fibre populations per voxel. FBA provides information regarding white matter structure for fibre bundles within a voxel through estimates of microstructure via local fibre density (FD), and morphometry via the fibre cross-section (FC) metric; their product, the fibre density and cross section (FDC), serves as a proxy of a fibre bundle's capacity to relay information [32]. This is of particular use in the neonatal brain where different white matter fibre populations within a voxel may be at different stages of development [33–35]. Given its key advantages over DTI, the FBA framework is increasingly adopted in studies of both typical and clinical populations (see review by Dhollander and colleagues [36].

The primary aim of the current study was to improve our understanding of the relationship between maternal depressive symptoms and developing white matter using advanced neuroimaging in the largest neonatal sample to date.

We hypothesised that higher maternal depressive symptoms (as measured during the prenatal or early postnatal period) are associated with differences in FD, FC, and FDC in the uncinate fasciculus and cingulum in the neonatal brain. This study expands upon previous work from our group [11], shifting the focus towards depression and expanding the research question to also include the cingulum. A hypothesis-driven tract-specific approach was employed, in line with previous fixel-based work (see [36]); a direction of effect was not specified due to lack of comparable measures and inconsistencies in the literature to date.

Our secondary aim was to investigate the relationship between maternal depressive symptoms, neonatal white matter, and child behaviour assessed at 18 months of age, using a similar mediation analysis strategy as that of Hay and colleagues [13]. We aimed to build on our recent work [37] which showed, in an overlapping sample, that higher maternal depressive symptoms were associated with toddlers' higher internalising and externalising behaviour and social-emotional difficulties. We hypothesised that tracts with significant relationships with maternal depressive symptoms are associated with childhood internalising and externalising behaviour, and social-emotional difficulties. Thirdly, we hypothesised that associations between maternal depressive symptoms and behavioural outcomes are mediated by white matter micro- and/or macrostructure.

To our knowledge, this is the first study using fixel-based fibre metrics to investigate the relationship between maternal depressive symptoms and neonatal white matter development, as well as the first study to include multi-shell MR data allowing us to perform both fixel-based and DTI analyses.

MATERIALS AND METHODS

Participants

Infants were recruited between March 2015 and March 2021 as part of the dHCP. Ethical approval was obtained from the National Research Ethics Committee (14/LO/1169) and written informed parental consent was provided for all participants prior to data collection. Participants were invited to take part in one or more of the following: foetal MRI scan(s), neonatal MRI scan(s), and neurodevelopmental assessment. The analysis reported in this study is based on neonatal diffusion MRI (dMRI) data which, at the time the analysis was conducted, comprised data for $n = 894$ scans. Scans were excluded for the following reasons: repeat scans ($n = 106$), absence of completed Edinburgh Postnatal Depression Scale (EPDS, $n = 100$), not singleton pregnancy ($n = 87$), missing or incomplete dMRI data ($n = 85$), failed dHCP image quality control (https://biomedia.github.io/dHCP-release-notes/qc.html) ($n = 21$), gestational age (GA) at birth under 32 weeks ($n = 46$), postmenstrual age (PMA) at scan under 37 weeks ($n = 11$), major incidental findings as determined by a paediatric neuroradiologist ($n = 22$, e.g., arterial ischemic infarcts, brain size <1st centile), failed visual image quality control ($n = 2$), no successful T2-weighted scan ($n = 1$). The final sample for the MRI analysis included $n = 413$ mother infant-dyads. A subset of $n = 311$ participants also participated in a neurodevelopmental assessment conducted between 17–24 months post-expected delivery date.

Maternal and infant characteristics

Maternal depressive symptoms were measured using the EPDS [38] at each study visit. The EPDS is a 10-item screening tool (total score range 0–30). A cut-off of 11 or more has been shown to maximise the sensitivity and specificity of screening for depressive symptoms [39], while a score of 13 or more can be used to indicate high-level symptoms. EPDS scores were included in the analysis if completed during pregnancy (i.e., at a visit for a foetal scan) or in the early postnatal period (i.e., at the time of the first neonatal scan), as these scores were more likely to be reflective of mood during the prenatal and early postnatal period. EPDS scores in our sample were available as follows: $n = 4$ only prenatal timepoints, $n = 289$ only postnatal timepoint, $n = 120$ both prenatal and postnatal timepoints. As the EPDS only asks about symptoms over the last 7 days, in cases where participants completed more than one EPDS questionnaire, the highest score was chosen. EPDS scores used in this analysis were collected at prenatal timepoints for $n = 55$ (median GA = 28.78 weeks,

Table 1. Maternal and infant characteristics.

	Characteristic	Whole sample ($n = 413$)	High EPDS ($n = 52$)	Low EPDS ($n = 361$)
Mother	EPDS, median (range)	5 (0–28)	13 (11–28)	4 (0–10)
	EPDS-3A, median (range)	3 (0–9); $n = 410$	6 (2–9); $n = 51$	2 (0–7); $n = 359$
	History poor MH, *N* (%) Yes	115 (27.8%)	27 (51.9%)	88 (24.4%)
	SSRI use, *N* (%) Yes	8 (1.9%)	3 (5.8%)	5 (1.4%)
	Age, years, median (range)	34 (17–46)	34 (24–42)	34 (17–46)
	IMD scores, median (range)	27.37 (1.55–61.37)	25.05 (5.06–46.99)	27.83 (1.55–61.37)
	quintile, *N* (%)			
	1 (least deprived)	21 (5.4%)	2 (4.1%)	19 (5.5%)
	2	32 (8.2%)	5 (10.2%)	27 (7.9%)
	3	69 (17.6%)	8 (16.3%)	61 (17.8%)
	4	163 (41.6%)	23 (46.9%)	140 (40.8%)
	5 (most deprived)	107 (27.3%); $n = 392$	11 (22.4%); $n = 49$	96 (28.0%); $n = 343$
	Smoking, *N* (%), Yes	12 (2.9%)	1 (1.9%)	11 (3.0 %)
	No	385 (93.2%)	47 (90.4%)	338 (93.6%)
	No, stopped	16 (3.9%)	4 (7.7%)	12 (3.3%)
	Alcohol, *N* (%), Yes	40 (9.7%); $n = 412$	4 (7.7%)	36 (10%); $n = 360$
	Substance use, *N* (%), Yes	2 (0.5%); $n = 412$	0 (0%)	2 (0.6%); $n = 360$
	Ethnicity, *N* (%)			
	White British/Irish	177 (49%)	14 (26.9%)	163 (45.2%)
	White Other	93 (22.5%)	16 (30.8%)	77 (21.3%)
	Asian/Asian British	46 (11.1%)	6 (11.5%)	40 (11.1%)
	Black/Black British	54 (13.1%)	10 (19.2%)	44 (12.2%)
	Mixed ethnic group	16 (3.9 %)	4 (7.7%)	12 (3.3%)
	Other	21 (5.1 %)	2 (3.8%)	19 (5.3%)
	Did not answer	6 (1.4%)	0 (0%)	6 (1.7%)
	BMI, median (range)	23.51 (16.87–43.55); $n = 407$	23.77 (17.78–41.66)	23.46 (16.87–43.55); $n = 355$
Infant	Sex, *N* (%) Male	223 (54%)	28 (53.8%)	195 (54%)
	Female	190 (46%)	24 (46.2%)	166 (46%)
	GA birth, weeks, median (range)	40 (32.14–42.29)	39.64 (32.29–42.29)	40 (32.14–42.29)
	PMA scan, weeks, median (range)	41.29 (36.57–44.71)	41.29 (36.71–44.14)	41.29 (36.57–44.71)
	Delivery			
	Spontaneous vaginal	174 (42.1%)	22 (42.3%)	152 (42.1%)
	Emergency C-Section (labour)	63 (15.3%)	11 (21.2%)	52 (14.4%)
	Emergency C-Section (not labour)	34 (8.2%)	7 (13.5%)	27 (7.5%)
	Elective C-Section	45 (10.9%)	2 (3.8%)	43 (11.9%)
	Instrumental – forceps	59 (14.3%)	8 (15.3%)	51 (14.1%)
	Instrumental – ventouse	38 (9.2%)	2 (3.8%)	36 (9.9%)

EPDS Edinburgh Postnatal Depression Scale, *MH* mental health, *SSRI* selective serotonin reuptake inhibitors, *IMD* index of multiple deprivation, *BMI* pre-pregnancy body mass index, *GA* gestational age at birth, *PMA* postmenstrual age.
No missing values unless otherwise indicated in the table.

range 22.00–39.57) and first postnatal timepoint for $n = 358$ (median GA = 41.14 weeks, range 36.57–44.71). EPDS-3A scores were also calculated and reported, with a threshold of 6 or more suggesting anxiety symptoms [40].

Maternal history of poor mental health (coded as a binary yes/no) was determined based on multiple sources including maternal self-report, maternity notes, and mental health records from South London and Maudsley NHS Foundation Trust (see Supplementary).

Sociodemographic characteristics and medical history for the mother-infant dyads were collected at enrolment (Table 1). As a proxy of socioeconomic status, the Index of Multiple Deprivation (IMD) was calculated from maternal postcode based on the 2019 IMD classification [41] with higher scores representing greater social deprivation. The relationship between infant GA at birth and PMA at scan is depicted in Fig. S7.

MR Imaging

Acquisition. High resolution MRI of the neonatal brain was acquired on a Philips Achieva 3 T system (Best, The Netherlands) using a dedicated 32-channel neonatal head coil and a neonatal positioning device [42]. Neonates were scanned during natural sleep and monitored throughout the scan (see Supplementary) whilst a paediatrician with experience in MRI was present.

The full dHCP protocol includes structural, functional, and diffusion imaging, but the current study is focused on the latter. Multi-shell High Angular Resolution Diffusion Imaging was acquired over 20 min using a protocol optimised for the neonatal brain [43, 44]. For all completed scans, each dataset contained 300 volumes of Echo Planar Imaging slices, sampled with four phase-encode directions on four shells with b-values of 0 ($n = 20$), 400 s/mm^2 ($n = 64$), 1000 s/mm^2 ($n = 88$) and 2600 s/mm^2 ($n = 128$). Acceleration of multiband 4, SENSE factor 1.2, and partial Fourier 0.86

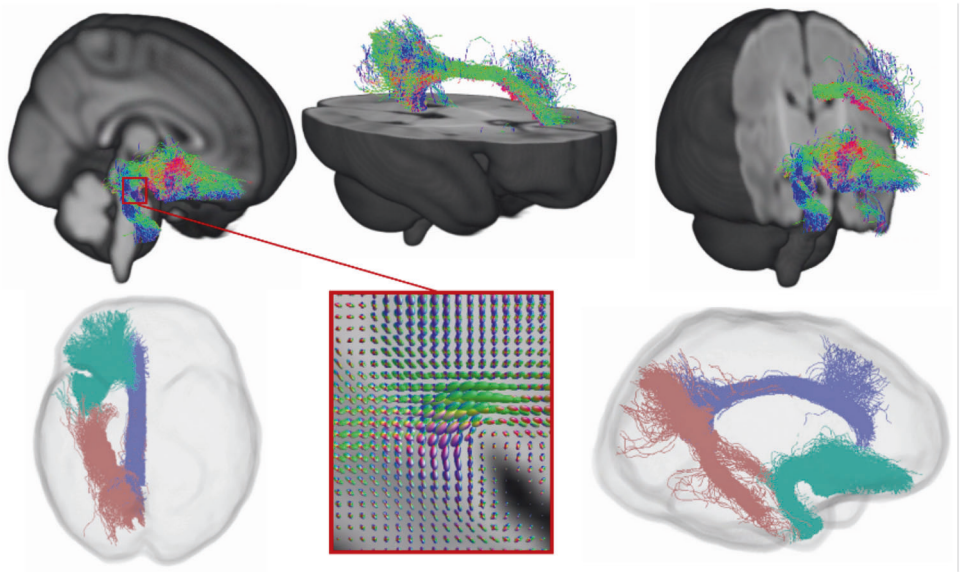

Fig. 1 Visual representation of the tracts in template space. The top row shows the location of the tracts, coloured by streamline orientation (blue: superior-inferior, red: left-right, green: anterior-posterior). On the bottom row, the middle image shows an example of fibre orientation distributions in a region of crossing fibres, while the left and right images represent "glass-brain" illustrations of the tracts of interest (pink: ventral cingulum, purple: dorsal cingulum, turquoise: uncinate fasciculus).

were used, with acquired resolution 1.5 × 1.5 mm, 3 mm slices with 1.5 mm overlap, and TR/TE of 3800/90 ms. Images were processed with denoising [45], Gibbs ringing suppression [46], motion and image distortion correction using slice-to-volume reconstruction to a 1.5 mm isotropic resolution [47], and inter-slice intensity inconsistency correction [48].

Pre-processing. The processing pipeline of the dMRI data follows that of the FBA framework but was adapted to account for the properties of neonatal tissue [34]. For all subjects, tissue-specific signal fingerprints (response functions) were estimated for single-fibre white matter and cerebrospinal fluid (CSF) using the Dhollander method [49], with an FA threshold of 0.15 for white matter and masks that exclude areas of CSF flow.

For group-analysis, response functions representative of free fluid and white matter diffusion signal at 44 weeks were calculated by averaging all CSF response functions and 21 white matter response functions from subjects aged 44.1 (SD 0.3) weeks. These group-average response functions were used to calculate maps of free water density and tissue Fibre Orientation Distributions (FODs) using multi-shell multi-tissue constrained spherical deconvolution [50, 51]. The estimated FODs were intensity normalised [52, 53] and conservative brain masks generated by intersecting masks generated in MRtrix3 [54] and by the brain extraction tool in FSL [55].

For group-analysis, a representative template was generated from the average of all subjects' normalised white matter FOD and free water density images transformed from native to the "Schuh dHCP extended atlas" 40-week anatomical template space [56]. These transformations are composite warps consisting of transformations released as part of the dHCP data release 3: a rigid-body subject-dMRI to subject-T2w (estimated with FSL flirt using a normalised mutual information metric), subject-T2w to age-matched T2-weighted template (estimated with nonlinear diffeomorphic multimodal registration of T2-weighted image and grey matter/white matter (GM/WM) tissue probability maps using the diffeomorphic symmetric image normalisation method (SyN) in the Advanced Normalisation Tools (ANTs) software package [57]) and week-to-week nonlinear transformations to the 40-week dHCP extended atlas template (estimated using the template T2-weighted images and SyN registration). The aggregate warps were estimated on a 1.3 isotropic grid, yielding a study-specific two-tissue template with the same resolution.

Each subject's normalised white matter FOD and fluid density images were jointly coregistered to the study specific template based on [58] using a normalised cross correlation metric, maximum spherical harmonics order $l_{max} = 2$ and a multi-resolution pyramid with 66 stages from 3.75 mm to 1.5 mm voxel size. FODs and masks were warped to the template space using cubic and linear interpolation, respectively.

All T2-weighted images were motion corrected and reconstructed to a 0.8 mm isotropic resolution [59], images were processed and segmented using the dHCP structural pipeline [60, 61] (see Supplementary).

Tractography in template space. Tractography of the left and right uncinate fasciculus, dorsal cingulum and ventral cingulum was performed on the white matter template using an anatomically constrained tractography (ACT) probabilistic algorithm with 50,000,000 seeds per tract (Fig. 1). ACT [62] was performed in template space using the draw-EM parcellation of the dHCP 40-week extended atlas template.

Regions of interest for tractography of the left and right uncinate fasciculus and dorsal and ventral cingulum (Table S1) were obtained from a neonatal version [63] of the anatomical automatic labelling (AAL) atlas [56, 64] adapted to the dHCP template. This was registered to the dHCP 40-week extended atlas template space using ANTs SyN [57].

Fixel-based fibre metrics. Tracts in template space were converted to fixel masks and mean FD, FC, and FDC were extracted across each tract for each baby, according to the MRtrix3 pipeline. Measures were averaged over all fixels. Apparent FD is, at high diffusion-weightings and subject to certain conditions [65], approximately proportional to the volume of the intra-axonal compartment. Sensitivity of apparent fibre density (AFD) to the tissue microstructure of individual fibre populations within a voxel ("fixels") can be achieved by segmenting the FOD lobes [66] and numerical integration over directions corresponding to the fixels. FC is a local measure of the change of a fixel's cross-sectional area due to warping to the joint template space (i.e., local expansion and contraction perpendicular to the bundle), with increases in this metric being thought to reflect an increase in the cross-sectional spatial extent occupied by a tract. FC was calculated from the subject-to-template warps estimated with mrregister and log-transformed (log(FC)) in accordance with the MRtrix3 pipeline recommendations. FDC is a composite metric reflecting both microstructural and morphological differences; it was calculated by multiplying FD and FC [67, 68].

Diffusion tensor imaging. To complement the information extracted from the FBA and enable comparison with previous literature, we undertook a secondary analysis using diffusion tensor imaging. FA and mean diffusivity (MD) maps for each infant were calculated from the $b = 0$ and $b = 1000$ shells of the dMRI data using MRtrix3. Tracts were warped from template space into native space for each infant, and mean DTI metrics for each tract in each infant were extracted and used for statistical analysis.

Child characteristics. A neurodevelopmental assessment was conducted at approximately 18 months of age. Outcomes of interest for the current

Table 2. Behavioural and cognitive outcomes in toddlers.

Characteristic	Whole sample ($n = 311$)	High EPDS ($n = 35$)	Low EPDS ($n = 276$)
IMD 18 months, median (range)	25.26 (1.55–61.37); $n = 292$	25.05 (5.06–53.18); $n = 33$	25.26 (1.55–61.37); $n = 259$
quintile, *N* (%)			
1 (least deprived)	28 (9.6%)	2 (6.1%)	26 (10.0%)
2	32 (11.0%)	3 (9.1%)	29 (11.2%)
3	52 (17.8%)	4 (12.1%)	48 (18.5%)
4	110 (37.7%)	15 (45.5%)	95 (36.7%)
5 (most deprived)	70 (24.0%)	9 (27.3%)	61 (23.6%)
Corrected age, months, median (range)	18 (17–24)	18 (17–24)	18 (17–24)
CBCL total T-score, median (range)	46 (28–69)	52 (37–66)	46 (28–69)
N (%), Normal (≤64)	301 (96.8%)	32 (91.4%)	269 (97.5%)
Borderline	10 (3.2%)	3 (8.6%)	7 (2.5%)
Clinical (≥70)	0 (0%)	0 (0%)	0 (0%)
CBCL Int. T-score, median (range)	43 (29–72)	49 (29–70)	43 (29–72)
CBCL Ext. T-score, median (range)	48 (28–70)	54 (28–65)	47 (28–70)
Q-CHAT Total, median (range)	29 (8–59)	32 (20–52)	28 (8–59)
N (%), Normal	272 (87.5%)	27 (77.1%)	245 (88.8%)
High (≥39)	39 (12.5%)	8 (22.9%)	31 (11.2%)
BSID-III Cog. Comp., median (range)	100 (70–125)	100 (70–120)	100 (70–125)
N (%), Normal (>85)	291 (93.6%)	32 (91.4%)	259 (93.8%)
Mild	20 (6.4%)	3 (8.6%)	17 (6.2%)
Mod/severe (<70)	0 (0%)	0 (0%)	0 (0%)
Home environment, median (range)	21 (7–28); $n = 305$	20 (12–28)	21 (7–28); $n = 270$
Dysfunctional parenting, median (range)	2.90 (1.43–4.20); $n = 308$	3.20 (2.37–4)	2.83 (1.43–4.20); $n = 273$

EPDS Edinburgh Postnatal Depression Scale, *IMD* index of multiple deprivation, *CBCL* Childhood Behaviour Checklist, *Q-CHAT* Quantitative Checklist for Autism in Toddlers, *Int* internalising, *Ext* externalising, *BSID-III Cog Comp* Bayley's cognitive composite score. Home environment = score on the Stimulating Parenting Scale, Dysfunctional parenting = score on the Parenting Scale.
No missing values unless otherwise indicated in the table. The cut-offs used to indicate high scores on the CBCL, Q-CHAT, and BSID-III as are per [69–71, 113] and are used for descriptive purposes only.

study included parent-reported behavioural outcomes measured using the Child Behaviour Checklist (CBCL) for ages 1.5 to 5 [69] and social-emotional abilities measured using the Quantitative Checklist for Autism in Toddlers (Q-CHAT, [70]. The CBCL includes 100 items and subscales for internalising behaviours (i.e., being withdrawn, somatic complaints, anxiety, depression, emotional reactivity) and externalising behaviours (i.e., attention problems, aggressive behaviours). The Q-CHAT includes 25 items evaluating social communication, as well as repetitive, stereotyped, and sensory behaviours. Cognitive development was assessed using the Bayley Scales of Infant and Toddler Development, 3rd Edition, 2006 (BSID-III, [71]), home environment was assessed with the Stimulating Parenting Scale [72] and dysfunctional parenting was assessed with the Parenting Scale [73] (Table 2).

Statistical analysis

Statistical analysis was performed using R version 4.1.1. (https://www.r-project.org/). The MR data utilised in this study is freely available: https://biomedia.github.io/dHCP-release-notes/. The R code used to analyse this data is available in the Supplement.

Regression. Multiple linear regressions were used to test the relationship between EPDS and brain measures, and the relationship between brain measures and child outcomes. Covariates were chosen a priori based on theoretical considerations and associations with variables of interest (See Supplementary).

First, using multiple linear regression, infant fixel-based fibre metrics were tested separately as dependent variables, with maternal EPDS and an EPDS-sex interaction as predictors. If the EPDS-sex interaction was not significant, it was excluded from the model and the analysis was rerun (as per [13]). The following covariates were also included in the models: GA at birth, PMA at scan, infant sex, maternal IMD at enrolment, maternal history of mental health (See Supplementary). For FDC and log(FC) models, ICV was also included as a covariate due to known associations with these metrics (e.g., [68]). Correction for multiple comparisons was performed using the False Discovery Rate (FDR) based on 6 tracts (i.e., left and right uncinate fasciculus, dorsal cingulum, ventral cingulum) and 3 values each (mean FD, log(FC), FDC), for a total of 18 comparisons.

Secondly, tracts with significant (after FDR correction) associations with maternal EPDS scores were analysed for associations with toddler behaviour. CBCL scores (internalising and externalising T scores) and Q-CHAT scores (total score) were tested separately as dependent variables, with the FBA metric and an FBA-sex interaction as predictors. If the FBA-sex interaction was not significant, it was excluded from the model and the analysis was rerun. The following covariates were also included in the models: infant sex, infant GA at birth, infant PMA at scan, maternal IMD at the 18-month assessment, child corrected age at assessment, BDSID-III cognitive score, and maternal age (see Supplementary).

Coefficients of determination (R^2) and F statistics (F) are reported for each regression model. Unstandardised coefficients (B), *t*-values (*t*) and uncorrected *p*-values (*p*) are reported for the EPDS or EPDS by sex variables. FDR-corrected (*q*) *p*-values are reported for all significant uncorrected *p*-values ($p < 0.05$).

Assumptions for regression were checked (linearity, homoscedasticity, independence, normality). Where assumptions for multiple regression were not met (see Supplementary), robust regression was performed using lmrob from the robustbase R package, which uses fast-S algorithms and heteroscedasticity and autocorrelation corrected (HAC) standard errors [74]. Robust regression is designed to be resistant to outlying observations and non-normality [75].

Mediation. A mediation analysis was conducted to investigate whether the relationship between maternal EPDS scores and toddler behaviour is

Table 3. Associations between maternal depressive symptoms and infant white matter.

		EPDS model			EPDS x Sex (female) model			Model fit	
Tract	**Metric**	**B**	***t***	***p* (*q*)**	**B**	***t***	***p* (*q*)**	**R^2**	**$F_{(df)}$**
UF-L	FD	0.0005	2.96	0.003 (.027)*				0.58	$F_{(6,385)} = 90.11$
	FDC				−0.0008	−2.62	0.009 (0.054)	0.73	$F_{(8,383)} = 134.1$
	Log(FC)	−0.0007	−1.33	0.183				0.72	$F_{(7,384)} = 143.4$
UF-R	FD	0.0006	3.04	0.003 (0.027)*				0.57	$F_{(6,385)} = 87.92$
	FDC	0.0004	2.30	0.022 (0.099)				0.74	$F_{(7,384)} = 158.3$
	Log(FC)	−0.0007	−1.37	0.171				0.74	$F_{(7,384)} = 157.6$
CD-L	FD	0.0003	1.66	0.099				0.34	$F_{(6,385)} = 35.1$
	FDC	0.0003	2.10	0.037 (0.133)				0.65	$F_{(7,384)} = 102.8$
	Log(FC)	0.0003	0.53	0.592				0.78	$F_{(7,384)} = 201.2$
CD-R	FD	0.0002	1.40	0.160				0.37	$F_{(6,385)} = 38.89$
	FDC	0.0003	1.71	0.088				0.66	$F_{(7,384)} = 110.6$
	Log(FC)	0.0003	0.52	0.607				0.74	$F_{(7,384)} = 157.9$
CV-L	FD	0.0002	1.23	0.218				0.40	$F_{(6,385)} = 45.04$
	FDC	0.0002	1.10	0.271				0.66	$F_{(7,384)} = 110$
	Log(FC)	−0.0001	−0.32	0.750				0.80	$F_{(7,384)} = 223.9$
CV-R	FD	0.0002	1.21	0.228				0.44	$F_{(6,385)} = 51.8$
	FDC	0.0001	0.91	0.362				0.68	$F_{(7,384)} = 120.3$
	Log(FC)	−0.00007	−0.16	0.870				0.79	$F_{(7,384)} = 214$

All models (R squared) were significant at $p < 0.001$. The R squared values reported are the adjusted ones, given that models have different numbers of variables. Covariates were gestational age at birth, postmenstrual age at scan, infant sex, maternal IMD at enrolment, maternal history of mental health. In addition, for FDC and log(FC) models, ICV was also included as a covariate. If EPDS by sex interaction was not significant, it was removed from the model and these cells are blank.

UF-L left uncinate fasciculus, *UF-R* right uncinate fasciculus, *CD-L* left dorsal cingulum, *CD-R* right dorsal cingulum, *CV-L* left ventral cingulum, *CV-R* right ventral cingulum, *B* = unstandardized coefficients, *q* = *p* values after FDR correction.

*Results that survive FDR correction for multiple comparisons.

mediated by changes in neonatal white matter. FBA metrics that were significantly associated with both EPDS scores and behaviour were selected for mediation analysis, with maternal EPDS scores as the predictor (X), FBA metrics as the mediator (M), and behaviour scores as the outcome variable (Y). Child age at neonatal scan and age at neurodevelopmental assessment were entered as covariates. Mediation was performed with the MeMoBootR package in R [76], with 5000 bootstrapped samples. This has been argued to be more powerful than the original causal steps mediation approach [77].

RESULTS

Mean values for the FBA and the DTI metrics for each tract are provided in Tables S2 and S3. For all tracts, FA was positively associated with FD (rho between 0.90 and 0.97, $p < 0.001$) and FDC (rho between 0.58 and 0.77, $p < 0.001$), and MD was negatively associated with FD (rho between −0.87 and −0.93, $p < 0.001$) and FDC (rho between −0.50 and −0.63, $p < 0.001$); both showed weak associations with log(FC) (Table S4).

Maternal depressive symptoms and neonatal white matter

Assumptions for multiple regressions were met for all models unless otherwise specified (See Supplementary). Results are summarised in Table 3.

Uncinate fasciculus. EPDS scores had a positive main effect on left uncinate fasciculus FD (B = 0.0005, t(385) = 2.958, $p = 0.003$) and right uncinate fasciculus FD (B = 0.0006, t(385) = 3.036, $p = 0.003$), so that infants of mothers with higher EPDS scores had higher FD (Fig. 2). Both relationships survived FDR correction for multiple comparisons (both $q = 0.027$), but the effect size was small compared to that of variables such as postmenstrual age at scan, and infant sex (Fig. 3, Table S12).

There was a significant EPDS by Sex interaction in left uncinate fasciculus FDC (B = −0.0008, t(383) = −2.622, $p = 0.009$), such that higher EPDS scores were associated with higher FDC in males (B = 0.0007, 95% CI [0.0003 − 0.0012]) but not females (B = −0.00006, 95% CI [−0.0005 − 0.0004]). EPDS also had a significant main effect on right uncinate fasciculus FDC (B = 0.0004, t(384) = 2.295, $p = 0.022$). These relationships did not survive correction for multiple comparisons ($q = 0.054$, $q = 0.099$).

There was no evidence for associations between EPDS and log(FC) for the uncinate fasciculus (see Supplementary).

Cingulum. EPDS scores had a positive main effect on left dorsal cingulum FDC (B = 0.0003, t(384) = 2.098, $p = 0.037$), but this relationship did not survive correction for multiple comparisons ($q = 0.133$). There were no associations with FD or log(FDC) (see Supplementary).

Sensitivity analyses. The analysis was repeated removing $n = 8$ participants whose mothers used SSRIs and removing $n = 3$ women who scored >20 on the EPDS, with comparable results (see Supplementary).

Exploratory analysis on diffusion tensor imaging data. There was a positive main association between maternal EPDS and infant FA in the left (B = 0.0003, t(384) = 2.705, $p = 0.007$) and right uncinate fasciculus (B = 0.0003, t(384) = 2.779, $p = 0.006$), and left dorsal cingulum (B = 0.0003, t(384) = 2.150, $p = 0.032$), and a negative association with MD in the right uncinate fasciculus (B = −0.000001, t(384) = −2.402, $p = 0.017$). These did not survive correction for multiple comparisons (*q* values: 0.063, 0.063, 0.102, 0.144, See Supplementary).

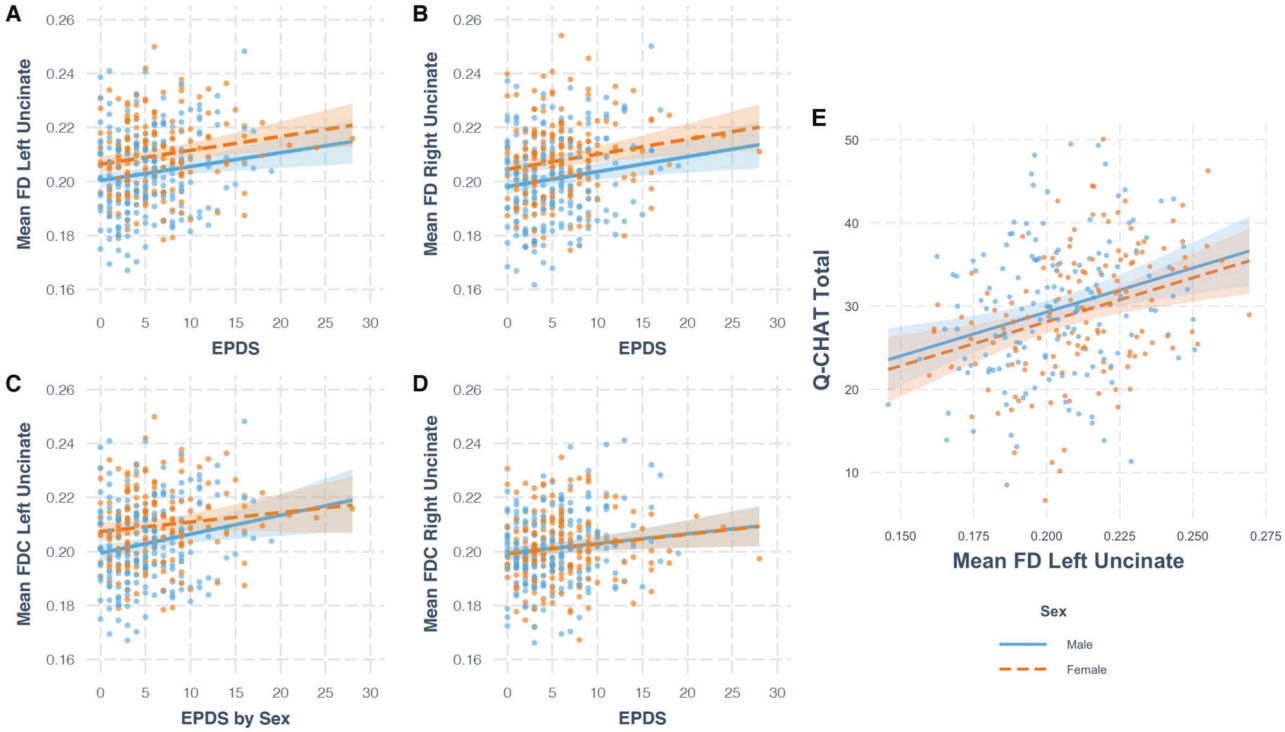

Fig. 2 Plots showing the relationships between variables of interest. A–D Contain plots showing the relationship between EPDS and white matter microstructure and macrostructure, controlling for effect of covariates. For mean FD left (**A**) and right (**B**) uncinate fasciculus and mean FDC right uncinate fasciculus (**D**), the main model is plotted. For mean FDC left uncinate fasciculus (**C**), the model with EPDS by Sex interaction is plotted. The relationship between EPDS and mean FD in the left and right uncinate fasciculus (**A**, **B**) survived FDR correction. **E** Contains a plot from robust regression, showing the relationship between mean FD in the left uncinate fasciculus and total Q-CHAT score, controlling for the effect of covariates.

Infant white matter microstructure and behaviour in toddlerhood

Results from robust regression suggested that infant FD in the uncinate fasciculus had a positive main effect on Q-CHAT scores ($B = 105.70$, $p = 0.0007$ for left, $B = 70.45$, $p = 0.020$ for right), so that infants with higher FD in this tract had higher Q-CHAT scores at 18 months (Fig. 2). The results for the left uncinate fasciculus survived FDR correction for multiple comparisons ($q = 0.004$), while results for the right uncinate fasciculus did not ($q = 0.06$). There were no FBA by sex interactions. There were no associations between infant FD in the uncinate fasciculus and CBCL internalising and externalising scores (see Supplementary). These results are consistent with those obtained using traditional regression methods (see Supplementary).

Sensitivity analyses. Results from a sensitivity analysis suggested comparable results for mean FD when controlling for postnatal home environment ($B = 107.45$, $p = 0.0006$ for left, and $B = 71.09$, $p = 0.020$ for right uncinate fasciculus), as well as when controlling for dysfunctional parenting ($B = 93.34$, $p = 0.002$ for left, and $B = 61.86$, $p = 0.036$ for right uncinate fasciculus).

Mediation

EPDS scores predicted total Q-CHAT scores, with $B = .342$, $t(307) = 3.003$, $p = 0.003$. However, there was no evidence that FD in the left uncinate fasciculus mediated the relationship between maternal EPDS and total Q-CHAT scores (Sobel test $z = 1.46$, $p = 0.143$, bootstrapped indirect effect $= 0.035$, $SE = 0.02$, 95% CI [−0.01−0.08]) (see Supplementary).

DISCUSSION

We used fixel-based fibre metrics to investigate the relationship between maternal depressive symptoms and neonatal brain development. We report, for the first time, that higher severity of maternal depressive symptoms is associated with higher fibre density (FD) in the neonatal uncinate fasciculus, when controlling for infant gestational age (GA) at birth, postmenstrual age (PMA) at scan, sex, maternal socioeconomic status, and maternal history of poor mental health. These results are strengthened by an exploratory analysis using diffusion tensor imaging, which suggests the same direction of effect (i.e., increased fractional anisotropy, FA and decreased mean diffusivity, MD). Further, higher FD in the uncinate fasciculus was also associated with social-emotional difficulties in toddlers. Results of a mediation analysis suggest that maternal depressive symptoms predict social-emotional difficulties, but there was no evidence that this relationship was mediated by uncinate fasciculus FD.

Our results are consistent with several previous dMRI studies which found increased FA and/or decreased diffusivity following exposure to maternal depression [8, 15], SSRI use [9, 78], cortisol [79] and paternal early life stress [80]. Nolvi and colleagues [15] reported that increased whole-brain FA moderated the association between maternal depression and infant reactivity. However, we provide the first evidence that maternal depressive symptoms are associated with density of fibres in the uncinate fasciculus, but not fibre bundle size, in the neonatal period. In studies of rats, exposure to early stress has been shown to lead to accelerated myelination. For example, in male juvenile rats, exposure to early stress leads to accelerated myelination in the basolateral amygdala [81]. It is possible maternal stress leads to accelerated axonal growth and myelination of the uncinate fasciculus, however this hypothesis requires further investigation.

Typically, increased FD, increased FA, and decreased MD during infancy suggest white matter maturation (e.g., increased axonal density) and are associated with positive outcomes [36, 68]. However, our findings may provide support for the

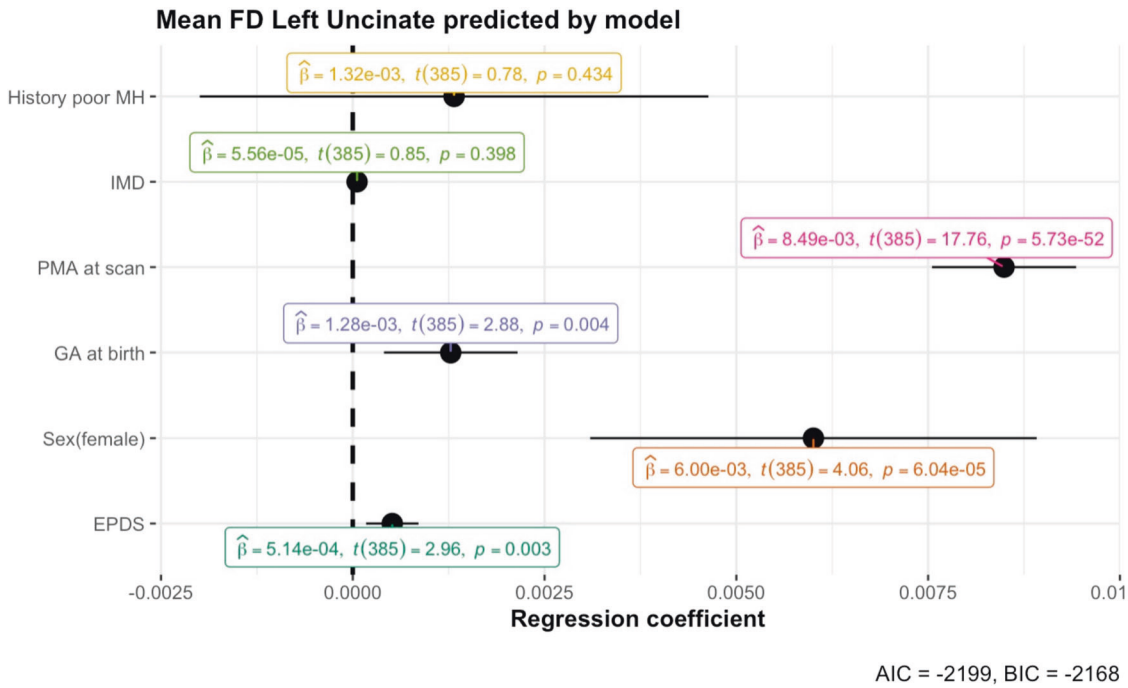

Fig. 3 Dot-and-whisker plot for the multiple linear regression model predicting mean FD in the left uncinate fasciculus. The black dots represent the regression coefficient estimate with 95% confidence intervals. The caption contains Akaike's Information Criterion (AIC) and the Bayesian Information Criterion (BIC), with smaller values indicating a better fit. For a model without EPDS, the AIC is −2193 and BIC is −2165, indicating a worst fit.

Stress Acceleration Hypothesis [82] which suggests that early adversity reprioritises developmental goals and leads to an accelerated developmental trajectory. The switch from growth to maturation [83] may offer a short-term survival advantage in a high-stress extrauterine environment (e.g., limbic areas often appear to be more mature following adversity), but may have adverse consequences in the longer term. Indeed, several structural MRI studies have reported prenatal-stress related increases in brain volumes [84–87]. Higher FA of the uncinate fasciculus in children has also been related to maternal unpredictability during infancy [88], and adolescents who had experienced increased early life trauma were more likely to be misclassified as adults based on their fronto-limbic microstructure [89]. It has been proposed that accelerated maturation in response to prenatal stress aims to compensate for reduced maternal investment [90]. This theory is also supported by animal studies showing that early stress is associated with precocious myelination [81] and enlarged volumes [91].

In a recent FBA study in children and adolescents [92], severity of early life stress was associated with more mature-appearing white matter structure (i.e., increased FDC), in tracts including the uncinate fasciculus. However, this was associated with fewer internalising problems in adolescence, but not late childhood [92], which the authors suggest this may be an adaptive response. More work is needed to understand longitudinal changes in brain development.

It is therefore essential to highlight the importance of the postnatal environment following exposure to prenatal stress. Early interventions have been suggested to improve outcomes for children at increased likelihood for autism [93, 94] and infants exposed to prenatal stress [95]. In one such study, cognitive behavioural therapy and augmentative communication were associated with higher uncinate fasciculus mean FA in autism [96], while in a preliminary study using FBA, FC was decreased in several tracts in offspring of women who received cognitive behavioural therapy [97]. Indeed, findings may be dependent on the time, duration, and intensity of the depressive symptoms. For example, it is possible that lower levels of stress are beneficial for white matter development, i.e., leading to increased FD, while higher levels of stress lead to decreased FD, in line with arguments that prenatal stress can be "both a risk and an opportunity factor" [98].

It is also possible that infants may be affected differently by prenatal stress based on pre-existing vulnerabilities. This may explain why, in a previous study conducted in extremely and very preterm babies, maternal stress was associated with higher uncinate fasciculus diffusivity [11]. Future research is needed to establish whether the effects of maternal stress are different for typically developing babies and those already at risk for adverse neurodevelopment. Further, future research should examine the role of maternal health and complications during labour and delivery.

Although overall there is variability with regards to the direction of effect [99], there is evidence suggesting that white matter development in autism may be characterised by abnormal early and/or accelerated maturation followed by decreased FA later on [100–102]. This is supported by our findings that increased FD in the uncinate fasciculus in infants is associated with social-emotional difficulties in toddlers. In a longitudinal study [19], young autistic children showed accelerated maturation of the uncinate fasciculus, which was associated with progression of social deficits. In a recent study in an overlapping sample [103], multi-modal cortical profiles in neonates predicted social-emotional performance at 18 months. Given the novelty of our findings, further research including longitudinal designs is required to replicate and better understand these results.

We identified a significant relationship between maternal depressive symptoms and microstructure in the neonatal uncinate fasciculus but not the cingulum bundle. Our results contrast reports that prenatal EPDS scores are associated altered cingulum microstructure in preschoolers [13] and that cingulum bundle FA in the neonatal period moderates the relationship between postpartum depression and infant reactivity at 6 months [15]. However, it is important to note that Hay and colleagues assessed cingulum bundle microstructure at 4 years of age and maternal

depression was measured at 3 and 6 months postpartum in Nolvi and colleagues' study [15]. These differences in age at exposure and age at assessment may account for the differing results. We have previously reported altered diffusivity in the uncinate fasciculus in infants born prematurely is associated with maternal stressful life events [11]. It is, therefore, possible that uncinate fasciculus microstructure in the neonatal period is associated with maternal stress, whereas cingulum bundle microstructure is affected at different time points. However, this hypothesis requires further investigation with longitudinal designs.

Compared to most previous research, our study included a larger number of women with high EPDS scores ($n = 52$). However, the EPDS only measures depressive symptoms over the previous 7 days, which means that elevated scores could have been transient in some women [104]. Future research should assesses a broader range of maternal psychological symptoms, more frequently, and across the whole perinatal and early postnatal period (e.g., [105]).

Future studies are also needed to further explore the interaction between foetal sex and exposure to maternal depression. Some prior studies have reported sex differences in the white matter of offspring exposed to prenatal stress [13, 78]. In our study, prenatal EPDS score was only associated with FDC in the left uncinate fasciculus in males, but this sex difference did not survive correction for multiple comparisons.

Increased maternal EPDS score during pregnancy or around the time of birth also predicted Q-CHAT scores in the first step of the mediation analysis. Children born to mothers with high EPDS scores were twice as likely to have social-emotional difficulties (22.9%) than those with low EPDS scores (11.2%) (Table 2). However, this relationship was not found to be mediated by uncinate fasciculus FD. Several factors may account for this. Firstly, it is likely that the biological mechanisms mediating the development of social-emotional traits are more complex than captured in our study design [106]. Secondly, our study lacks information about postnatal mental health, so it is possible that the observed effects may be related to postnatal stress [107]. Further, it is possible that maternal postnatal depressive symptoms may affect the reporting of offspring behaviour, in line with the depression-distortion hypothesis [108, 109]. Future research should control for maternal postnatal mental health and ideally complement parent-reported measures of behaviour with teacher reports and observational measures.

It is unclear why in our study there were no associations with CBCL scores. One possibility is that this is related to the uncertainty of differentiating between normative behaviours and psychopathology at such an early age. However, the CBCL has good validity in infancy and toddlerhood and satisfactory predictive validity [69, 110]. With regards to the Q-CHAT, reports from parents of autistic children often mention concerns around the first year of life [111, 112]. However, it is important to note that the Q-CHAT has been suggested to have low predictive validity and the appearance of early social-emotional difficulties does not imply a later autism diagnosis [113], highlighting the importance of longitudinal study designs. In addition, Goh and colleagues [114] reported that higher maternal depressive symptoms were associated with a small but significant increase in maternal-reported QCHAT socio-communicative, but not behavioural, traits in healthy toddlers. Although we did not measure maternal depressive symptoms at follow-up, it is possible that mothers with persistent depressive symptoms were more likely to report socio-communicative difficulties measured with the QCHAT than behavioural difficulties on the CBCL. It is also possible that offspring are affected differently by prenatal depression based on other factors such as genetic susceptibility [115]. Future studies should aim to capture individual variability in outcomes, which could be achieved using different analysis techniques such as normative modelling [116].

To our knowledge, this represents the largest study investigating the relationship between maternal depressive symptoms and neonatal white matter, as well as the first such study to use fixel-based fibre metrics, which increase microstructural and spatial specificity [36]. We encourage future research to replicate these results, addressing the limitations outlined above and including even larger samples [117]. Our findings have important implications for clinical practice, as a better understanding of how maternal depressive symptoms can impact offspring brain and behaviour can help inform future interventions and ensure more positive outcomes for mother and child.

REFERENCES

1. O'Donnell KJ, Glover V, Barker ED, O'Connor TG. The persisting effect of maternal mood in pregnancy on childhood psychopathology. Dev Psychopathol. 2014;26:393–403.
2. Lautarescu A, Craig MC, Glover V. (2020): Chapter Two - Prenatal stress: Effects on fetal and child brain development. In: Clow A, Smyth N, editors. International Review of Neurobiology, vol. 150. Academic Press, pp 17–40.
3. Scheinost D, Sinha R, Cross SN, Kwon SH, Sze G, Constable RT, et al. Does prenatal stress alter the developing connectome? Pediatr Res. 2017;81:214–26.
4. Kelly CJ, Hughes EJ, Rutherford MA, Counsell SJ. Advances in neonatal MRI of the brain: from research to practice. Arch Dis Child - Educ Pract Ed. 2019;104:106–10.
5. Graham RM, Jiang L, McCorkle G, Bellando BJ, Sorensen ST, Glasier CM, et al. Maternal anxiety and depression during late pregnancy and newborn brain white matter development. Am J Neuroradiol. 2020;41:1908–15.
6. Rifkin-Graboi A, Bai J, Chen H, Hameed WB, Sim LW, Tint MT, et al. Prenatal maternal depression associates with microstructure of right amygdala in neonates at birth. Biol Psychiatry. 2013;74:837–44.
7. Rifkin-Graboi A, Meaney MJ, Chen H, Bai J, Hameed WB, Tint MT, et al. Antenatal maternal anxiety predicts variations in neural structures implicated in anxiety disorders in newborns. J Am Acad Child Adolesc Psychiatry. 2015;54:313–21.e2.
8. Borchers L, Dennis E, King L, Humphreys K, Gotlib I. The effects of maternal depression on infant white matter organization and social-emotional development: a longitudinal study. Biol Psychiatry. 2020;87:S106.
9. Podrebarac SK, Duerden EG, Chau V, Grunau RE, Synnes A, Oberlander TF, et al. Antenatal exposure to antidepressants is associated with altered brain development in very preterm-born neonates. Neuroscience. 2017;342:252–62.
10. Dennis EL, Singh A, Corbin CK, Jahanshad N, Ho TC, King LS, et al. Associations between maternal depression and infant fronto-limbic connectivity. 2019 IEEE 16th International Symposium on Biomedical Imaging (ISBI 2019). 2019;126–30.
11. Lautarescu A, Pecheva D, Nosarti C, Nihouarn J, Zhang H, Victor S, et al. Maternal prenatal stress is associated with altered uncinate fasciculus microstructure in premature neonates. Biol Psychiatry. 2020;87:559–69.
12. Sarkar S, Craig MC, Dell'Acqua F, O'Connor TG, Catani M, Deeley Q, et al. Prenatal stress and limbic-prefrontal white matter microstructure in children aged 6–9 years: a preliminary diffusion tensor imaging study. World J Biol Psychiatry. 2014;15:346–52.
13. Hay RE, Reynolds JE, Grohs MN, Paniukov D, Giesbrecht GF, Letourneau N, et al. Amygdala-prefrontal structural connectivity mediates the relationship between prenatal depression and behavior in preschool boys. J Neurosci. 2020;40:6969–77.
14. Marečková K, Klasnja A, Bencurova P, Andrýsková L, Brázdil M, Paus T. Prenatal stress, mood, and gray matter volume in young adulthood. Cereb Cortex. 2019;29:1244–50.
15. Nolvi S, Tuulari JJ, Lavonius T, Scheinin NM, Lehtola SJ, Lavonius M, et al. Newborn white matter microstructure moderates the association between maternal postpartum depressive symptoms and infant negative reactivity. Soc Cogn Affect Neurosci. 2020;15:649–60.
16. Bracht T, Linden D, Keedwell P. A review of white matter microstructure alterations of pathways of the reward circuit in depression. J Affect Disord. 2015;187:45–53.
17. Bubb EJ, Metzler-Baddeley C, Aggleton JP. The cingulum bundle: Anatomy, function, and dysfunction. Neurosci Biobehav Rev. 2018;92:104–27.
18. Coad BM, Postans M, Hodgetts CJ, Muhlert N, Graham KS, Lawrence AD. Structural connections support emotional connections: Uncinate Fasciculus microstructure is related to the ability to decode facial emotion expressions. Neuropsychologia. 2020;145:106562.
19. Li Y, Zhou Z, Chang C, Qian L, Li C, Xiao T, et al. Anomalies in uncinate fasciculus development and social defects in preschoolers with autism spectrum disorder. BMC Psychiatry. 2019;19:399.

20. Samson AC, Dougherty RF, Lee IA, Phillips JM, Gross JJ, Hardan AY. White matter structure in the uncinate fasciculus: Implications for socio-affective deficits in Autism Spectrum Disorder. Psychiatry Research: Neuroimaging 255:66–74.
21. Brenner RG, Smyser CD, Lean RE, Kenley JK, Smyser TA, Cyr PEP, et al. Microstructure of the dorsal anterior cingulum bundle in very preterm neonates predicts the preterm behavioral phenotype at 5 years of age. Biol Psychiatry. 2021;89:433–42.
22. Solso S, Xu R, Proudfoot J, Hagler DJ, Campbell K, Venkatraman V, et al. DTI provides evidence of possible axonal over-connectivity in frontal lobes in ASD toddlers. Biol Psychiatry. 2016;79:676–84.
23. Kanel D, Vanes LD, Pecheva D, Hadaya L, Falconer S, Counsell SJ, et al. Neonatal white matter microstructure and emotional development during the preschool years in children who were born very preterm. eNeuro. 2021;8:ENEURO.0546-20.2021.
24. Gerardin P, Wendland J, Bodeau N, Galin A, Bialobos S, Tordjman S, et al. Depression during pregnancy: is the developmental impact earlier in boys? A prospective case-control study. J Clin Psychiatry. 2011;72:378–87.
25. Graham AM, Rasmussen JM, Entringer S, Ben Ward E, Rudolph MD, Gilmore JH, et al. Maternal cortisol concentrations during pregnancy and sex-specific associations with neonatal amygdala connectivity and emerging internalizing behaviors. Biol Psychiatry. 2019;85:172–81.
26. Graham AM, Rasmussen JM, Rudolph MD, Heim CM, Gilmore JH, Styner M, et al. Maternal systemic interleukin-6 during pregnancy is associated with newborn amygdala phenotypes and subsequent behavior at 2 years of age. Biol Psychiatry. 2018;83:109–19.
27. Scheinost D, Spann MN, McDonough L, Peterson BS, Monk C. Associations between different dimensions of prenatal distress, neonatal hippocampal connectivity, and infant memory [no. 8]. Neuropsychopharmacology. 2020;45:1272–9.
28. Moog NK, Nolvi S, Kleih TS, Styner M, Gilmore JH, Rasmussen JM, et al. Prospective association of maternal psychosocial stress in pregnancy with newborn hippocampal volume and implications for infant social-emotional development. Neurobiol Stress. 2021;15:100368.
29. Pierpaoli C, Jezzard P, Basser PJ, Barnett A, Di Chiro G. Diffusion tensor MR imaging of the human brain. Radiology. 1996;201:637–48.
30. Lanyon LJ. Diffusion tensor imaging: Structural connectivity insights, limitations and future directions. Neuroimaging Methods. 2012;1:137–62.
31. Jeurissen B, Leemans A, Tournier J-D, Jones DK, Sijbers J. Investigating the prevalence of complex fiber configurations in white matter tissue with diffusion magnetic resonance imaging: prevalence of multifiber voxels in WM. Hum Brain Mapp. 2013;34:2747–66.
32. Raffelt DA, Tournier J-D, Smith RE, Vaughan DN, Jackson G, Ridgway GR, et al. Investigating white matter fibre density and morphology using fixel-based analysis. NeuroImage. 2017;144:58–73.
33. Ouyang M, Dubois J, Yu Q, Mukherjee P, Huang H. Delineation of early brain development from fetuses to infants with diffusion MRI and beyond. Neuroimage. 2019;185:836–50.
34. Pietsch M, Christiaens D, Hutter J, Cordero-Grande L, Price AN, Hughes E, et al. A framework for multi-component analysis of diffusion MRI data over the neonatal period. NeuroImage. 2019;186:321–37.
35. Wilson S, Pietsch M, Cordero-Grande L, Price AN, Hutter J, Xiao J, et al. Development of human white matter pathways in utero over the second and third trimester. Proc Natl Acad Sci USA. 2021;118:e2023598118.
36. Dhollander T, Clemente A, Singh M, Boonstra F, Civier O, Duque JD, et al. Fixel-based analysis of diffusion MRI: methods, applications, challenges and opportunities. NeuroImage. 2021;241:118417.
37. Kleine I, Vamvakas G, Lautarescu A, Falconer S, Chew A, Counsell SJ, et al. Postnatal maternal depressive symptoms and behavioural outcomes in term- and preterm-born toddlers. medRxiv. 2021.09.21.21263881.
38. Cox JL, Holden JM, Sagovsky R. Detection of postnatal depression: development of the 10-item edinburgh postnatal depression scale. Br J Psychiatry. 1987;150:782–6.
39. Levis B, Negeri Z, Sun Y, Benedetti A, Thombs BD. Accuracy of the Edinburgh Postnatal Depression Scale (EPDS) for screening to detect major depression among pregnant and postpartum women: systematic review and meta-analysis of individual participant data. BMJ. 2020;371:m4022.
40. Matthey S. Using the Edinburgh Postnatal Depression Scale to screen for anxiety disorders. Depression Anxiety. 2008;25:926–31.
41. McLennan D, Noble S, Noble M, Plunkett E, Wright G, Gutacker N. English Indices of Deprivation 2019: technical report. Ministry of Housing, Communities and Local Government. 2019;117.
42. Hughes EJ, Winchman T, Padormo F, Teixeira R, Wurie J, Sharma M, et al. A dedicated neonatal brain imaging system: A Dedicated Neonatal Brain Imaging System. Magn Reson Med. 2017;78:794–804.
43. Hutter J, Tournier JD, Price AN, Cordero-Grande L, Hughes EJ, Malik S, et al. Time-efficient and flexible design of optimized multishell HARDI diffusion. Magn Reson Med. 2018;79:1276–92.
44. Tournier J, Christiaens D, Hutter J, Price AN, Cordero-Grande L, Hughes E, et al. A data-driven approach to optimising the encoding for multi-shell diffusion MRI with application to neonatal imaging. NMR Biomed. 2020;33:1–18.
45. Cordero-Grande L, Christiaens D, Hutter J, Price AN, Hajnal JV. Complex diffusion-weighted image estimation via matrix recovery under general noise models. NeuroImage. 2019;200:391–404.
46. Kellner E, Dhital B, Kiselev VG, Reisert M. Gibbs-ringing artifact removal based on local subvoxel-shifts. Magn Reson Med. 2016;76:1574–81.
47. Christiaens D, Cordero-Grande L, Pietsch M, Hutter J, Price AN, Hughes EJ, et al. Scattered slice SHARD reconstruction for motion correction in multi-shell diffusion MRI. NeuroImage. 2021;225:117437.
48. Pietsch M, Christiaens D, Hajnal JV, Tournier J-D. dStripe: slice artefact correction in diffusion MRI via constrained neural network. bioRxiv. 2020.10.20.347518.
49. Dhollander T, Mito R, Raffelt D, Connelly A. Improved white matter response function estimation for 3-tissue constrained spherical deconvolution. Proceeds Int Soc Magn Reson Med. 2019;27:555.
50. Jeurissen B, Tournier J-D, Dhollander T, Connelly A, Sijbers J. Multi-tissue constrained spherical deconvolution for improved analysis of multi-shell diffusion MRI data. NeuroImage. 2014;103:411–26.
51. Tournier J-D, Yeh C-H, Calamante F, Cho K-H, Connelly A, Lin C-P. Resolving crossing fibres using constrained spherical deconvolution: Validation using diffusion-weighted imaging phantom data. NeuroImage. 2008;42:617–25.
52. Dhollander T, Tabarra R, Rosnarho-Tornstrand J, Tournier J-D, Raffelt D, Connelly A. Multi-tissue log-domain intensity and inhomogeneity normalisation for quantitative apparent fibre density. Proceeds Int Soc Magn Reson Med. 2021;29:2472.
53. Raffelt D, Dhollander T, Tournier J-D, Tabbara R, Smith R, Pierre E, et al. Bias field correction and intensity normalisation for quantitative analysis of apparent fibre density. In Proc Intl Soc Mag Reson Med. 2017;25:541.
54. Tournier J-D, Smith R, Raffelt D, Tabbara R, Dhollander T, Pietsch M, et al. MRtrix3: A fast, flexible and open software framework for medical image processing and visualisation. NeuroImage. 2019;202:116137.
55. Smith SM. Fast robust automated brain extraction. Hum Brain Mapp. 2002;17:143–55.
56. Schuh A, Makropoulos A, Robinson EC, Cordero-Grande L, Hughes E, Hutter J, et al. Unbiased construction of a temporally consistent morphological atlas of neonatal brain development. bioRxiv. 2018. Retrieved August 4, 2021, from http://biorxiv.org/lookup/doi/10.1101/251512.
57. Avants BB, Epstein CL, Grossman M, Gee JC. Symmetric diffeomorphic image registration with cross-correlation: Evaluating automated labeling of elderly and neurodegenerative brain. Med Image Anal. 2008;12:26–41.
58. Raffelt D, Tournier J-D, Fripp J, Crozier S, Connelly A, Salvado O. Symmetric diffeomorphic registration of fibre orientation distributions. NeuroImage. 2011;56:1171–80.
59. Cordero-Grande L, Hughes EJ, Hutter J, Price AN, Hajnal JV. Three-dimensional motion corrected sensitivity encoding reconstruction for multi-shot multi-slice MRI: Application to neonatal brain imaging. Magn Reson Med. 2018;79:1365–76.
60. Makropoulos A, Gousias IS, Ledig C, Aljabar P, Serag A, Hajnal JV, et al. Automatic whole brain mri segmentation of the developing neonatal brain. IEEE Trans Med Imaging. 2014;33:1818–31.
61. Makropoulos A, Robinson EC, Schuh A, Wright R, Fitzgibbon S, Bozek J, et al. The developing human connectome project: A minimal processing pipeline for neonatal cortical surface reconstruction. NeuroImage. 2018;173:88–112.
62. Smith RE, Tournier J-D, Calamante F, Connelly A. Anatomically-constrained tractography: Improved diffusion MRI streamlines tractography through effective use of anatomical information. NeuroImage. 2012;62:1924–38.
63. Shi F, Yap P-T, Wu G, Jia H, Gilmore JH, Lin W, et al. Infant Brain Atlases from Neonates to 1- and 2-Year-Olds ((H. Okazawa, editor)). PLoS ONE. 2011;6:e18746.
64. Tzourio-Mazoyer N, Landeau B, Papathanassiou D, Crivello F, Etard O, Delcroix N, et al. Automated anatomical labeling of activations in SPM using a macroscopic anatomical parcellation of the MNI MRI single-subject brain. NeuroImage. 2002;15:273–89.
65. Raffelt D, Tournier J-D, Rose S, Ridgway GR, Henderson R, Crozier S, et al. Apparent Fibre Density: A novel measure for the analysis of diffusion-weighted magnetic resonance images. NeuroImage. 2012;59:3976–94.
66. Pecheva D, Tournier J-D, Pietsch M, Christiaens D, Batalle D, Alexander DC, et al. Fixel-based analysis of the preterm brain: Disentangling bundle-specific white matter microstructural and macrostructural changes in relation to clinical risk factors. NeuroImage: Clin. 2019;23:101820.
67. Burley DT, Genc S, Silk TJ. Childhood conduct problems are associated with reduced white matter fibre density and morphology. J Affect Disord. 2021;281:638–45.
68. Genc S, Malpas CB, Gulenc A, Sciberras E, Efron D, Silk TJ, et al. Longitudinal patterns of white matter fibre density and morphology in children are associated with age and pubertal stage. Developmental Cogn Neurosci. 2020;45:100853.

69. Achenbach T, Rescorla LA. Manual for the ASEBA Preschool Forms and Profiles, vol. 30. Burlington, VT: University of Vermont, Research centre for children, youth and families.2000.
70. Allison C, Baron-Cohen S, Wheelwright S, Charman T, Richler J, Pasco G, et al. The Q-CHAT (Quantitative CHecklist for Autism in Toddlers): a normally distributed quantitative measure of autistic traits at 18–24 months of age: preliminary report. J Autism Developmental Disord. 2008;38:1414–25.
71. Bayley N. Bayley scales of infant and toddler development: Bayley-III. 2006. Harcourt Assessment, San Antonio, TX.
72. Wolke D, Jaekel J, Hall J, Baumann N. Effects of sensitive parenting on the academic resilience of very preterm and very low birth weight adolescents. J Adolesc Health. 2013;53:642–7.
73. Arnold DS, O'Leary SG, Wolff LS, Acker MM. The Parenting Scale: A measure of dysfunctional parenting in discipline situations. Psychological Assess. 1993;5:137–44.
74. Maechler M, Rousseuw P, Croux C, Todorov V, Ruckstuhl A, Salibian-Barrera M, et al. Robustbase: Basic robust statistics. 2021. http://robustbase.r-forge.r-project.org/.
75. Lourenço VM, Pires AM, Kirst M. Robust linear regression methods in association studies. Bioinformatics. 2011;27:815–21.
76. Buchanan EM. MeMoBootR Version: 0.0 0.4000 [Computer Program]. 2018. Available at: https://github.com/doomlab/MeMoBootR.
77. Baron RM, Kenny DA. The moderator–mediator variable distinction in social psychological research: Conceptual, strategic, and statistical considerations. J Personal Soc Psychol. 1986;51:1173–82.
78. Campbell KSJ, Williams LJ, Bjornson BH, Weik E, Brain U, Grunau RE, et al. Prenatal antidepressant exposure and sex differences in neonatal corpus callosum microstructure. Developmental Psychobiol. 2021. https://doi.org/10.1002/dev.22125.
79. Stoye DQ, Blesa M, Sullivan G, Galdi P, Lamb GJ, Black GS, et al. Maternal cortisol is associated with neonatal amygdala microstructure and connectivity in a sexually dimorphic manner. bioRxiv. 2020.06.16.154922.
80. Karlsson H, Merisaari H, Karlsson L, Scheinin NM, Parkkola R, Saunavaara J, et al. Association of cumulative paternal early life stress with white matter maturation in newborns. JAMA Netw Open. 2020;3:e2024832–e2024832.
81. Ono M, Kikusui T, Sasaki N, Ichikawa M, Mori Y, Murakami-Murofushi K. Early weaning induces anxiety and precocious myelination in the anterior part of the basolateral amygdala of male Balb/c mice. Neuroscience. 2008;156:1103–10.
82. Callaghan BL, Tottenham N. The Stress Acceleration Hypothesis: effects of early-life adversity on emotion circuits and behavior. Curr Opin Behav Sci. 2016;7:76–81.
83. Bath KG, Manzano-Nieves G, Goodwill H. Early life stress accelerates behavioral and neural maturation of the hippocampus in male mice. Hormones Behav. 2016;82:64–71.
84. Acosta H, Kantojärvi K, Tuulari JJ, Lewis JD, Hashempour N, Scheinin NM, et al. Sex-specific association between infant caudate volumes and a polygenic risk score for major depressive disorder. J Neurosci Res. 2020;98:2529–40.
85. Lugo-Candelas C, Cha J, Hong S, Bastidas V, Weissman M, Fifer WP, et al. Associations between brain structure and connectivity in infants and exposure to selective serotonin reuptake inhibitors during pregnancy. JAMA Pediatrics. 2018;172:525–33.
86. Qiu A, Shen M, Buss C, Chong Y-S, Kwek K, Saw S-M, et al. Effects of antenatal maternal depressive symptoms and socio-economic status on neonatal brain development are modulated by genetic risk. Cereb Cortex. 2017;27:3080–92.
87. Spann MN, Bansal R, Hao X, Rosen TS, Peterson BS. Prenatal socioeconomic status and social support are associated with neonatal brain morphology, toddler language and psychiatric symptoms. Child Neuropsychol. 2020;26:170–88.
88. Granger SJ, Glynn LM, Sandman CA, Small SL, Obenaus A, Keator DB, et al. Aberrant maturation of the uncinate fasciculus follows exposure to unpredictable patterns of maternal signals. J Neurosci. 2021;41:1242–50.
89. Gur RE, Moore TM, Rosen AFG, Barzilay R, Roalf DR, Calkins ME, et al. Burden of environmental adversity associated with psychopathology, maturation, and brain behavior parameters in youths. JAMA Psychiatry. 2019;76:966–75.
90. Berghänel A, Heistermann M, Schülke O, Ostner J. Prenatal stress accelerates offspring growth to compensate for reduced maternal investment across mammals. Proc Natl Acad Sci. 2017;114:E10658–E10666.
91. Coplan JD, Fathy HM, Jackowski AP, Tang CY, Perera TD, Mathew SJ, et al. Early life stress and macaque amygdala hypertrophy: preliminary evidence for a role for the serotonin transporter gene. Front Behavioral Neurosci. 2014. https://doi.org/10.3389/fnbeh.2014.00342.
92. Chahal R, Kirshenbaum JS, Ho TC, Mastrovito D, Gotlib IH. Greater age-related changes in white matter morphometry following early life stress: Associations with internalizing problems in adolescence. Developmental Cogn Neurosci. 2021;47:100899.
93. Dawson G, Jones EJH, Merkle K, Venema K, Lowy R, Faja S, et al. Early behavioral intervention is associated with normalized brain activity in young children with autism. J Am Acad Child Adolesc Psychiatry. 2012;51:1150–9.
94. Green J, Pickles A, Pasco G, Bedford R, Wan MW, Elsabbagh M, et al. Randomised trial of a parent-mediated intervention for infants at high risk for autism: longitudinal outcomes to age 3 years. J Child Psychol Psychiatry. 2017;58:1330–40.
95. Antonelli MC, Frasch MG, Rumi M, Sharma R, Zimmermann P, Molinet MS, et al. Early biomarkers and intervention programs for the infant exposed to prenatal stress. Current Neuropharmacol. 2021. 19. Retrieved August 3, 2021, from http://arxiv.org/abs/2005.05787.
96. Pardini M, Elia M, Garaci FG, Guida S, Coniglione F, Krueger F, et al. Long-term cognitive and behavioral therapies, combined with augmentative communication, are related to uncinate fasciculus integrity in autism. J Autism Developmental Disord. 2012;42:585–92.
97. Bleker LS, Milgrom J, Parker D, Gemmill AW, Holt CJ, Connelly A, et al. Brain magnetic resonance imaging findings in children after antenatal maternal depression treatment, a longitudinal study built on a pilot randomized controlled trial [no. 10]. Int J Environ Res Public Health. 2019;16:1816.
98. Hartman S, Freeman SM, Bales KL, Belsky J. Prenatal stress as a risk—and an opportunity—factor. Psychological Sci. 2018;29:572–80.
99. Ameis SH, Catani M. Altered white matter connectivity as a neural substrate for social impairment in Autism Spectrum Disorder. Cortex. 2015;62:158–81.
100. Ben Bashat D, Kronfeld-Duenias V, Zachor DA, Ekstein PM, Hendler T, Tarrasch R, et al. Accelerated maturation of white matter in young children with autism: A high b value DWI study. NeuroImage. 2007;37:40–47.
101. Wolff JJ, Gu H, Gerig G, Elison JT, Styner M, Gouttard S, et al. Differences in white matter fiber tract development present from 6 to 24 months in infants with autism. Am J Psychiatry. 2012;169:589–600.
102. Xiao Z, Qiu T, Ke X, Xiao X, Xiao T, Liang F, et al. Autism spectrum disorder as early neurodevelopmental disorder: evidence from the brain imaging abnormalities in 2–3 years old toddlers. J Autism Developmental Disord. 2014;44:1633–40.
103. Fenchel D, Dimitrova R, Robinson EC, Batalle D, Chew A, Falconer S, et al. Neonatal multi-modal cortical profiles predict 18-month developmental outcomes. Developmental Cogn Neurosci. 2022;54:101103.
104. Agostini F, Matthey S, Minelli M, Dellabartola S, Bonapace S. Transient vs enduring distress in late pregnancy using the EPDS: a brief longitudinal exploratory study. J Reprod Infant Psychol. 2019;37:513–26.
105. Park M, Brain U, Grunau RE, Diamond A, Oberlander TF. Maternal depression trajectories from pregnancy to 3 years postpartum are associated with children's behavior and executive functions at 3 and 6 years. Arch Women's Ment Health. 2018;21:353–63.
106. Happé F, Ronald A, Plomin R. Time to give up on a single explanation for autism. Nat Neurosci. 2006;9:1218–20.
107. Murray L, Cooper P, Fearon P. Parenting difficulties and postnatal depression: implications for primary healthcare assessment and intervention [no. 11]. Community Practitioner. 2014;87:34–38.
108. Müller JM, Romer G, Achtergarde S. Correction of distortion in distressed mothers' ratings of their preschool-aged children's Internalizing and Externalizing scale score. Psychiatry Res. 2014;215:170–5.
109. Wesselhoeft R, Davidsen K, Sibbersen C, Kyhl H, Talati A, Andersen MS, et al. Maternal prenatal stress and postnatal depressive symptoms: discrepancy between mother and teacher reports of toddler psychological problems. Soc Psychiatry Psychiatr Epidemiol. 2021;56:559–70.
110. Zeijl JV, Mesman J, Stolk MN, Alink LRA, IJzendoorn MHV, Bakermans-Kranenburg MJ, et al. Terrible ones? Assessment of externalizing behaviors in infancy with the Child Behavior Checklist. J Child Psychol Psychiatry. 2006;47:801–10.
111. Chawarska K, Paul R, Klin A, Hannigen S, Dichtel LE, Volkmar F. Parental recognition of developmental problems in toddlers with autism spectrum disorders. J Autism Developmental Disord. 2007;37:62–72.
112. Talbott MR, Nelson CA, Tager-Flusberg H. Diary reports of concerns in mothers of infant siblings of children with autism across the first year of life. J Autism Developmental Disord. 2015;45:2187–99.
113. Allison C, Matthews FE, Ruta L, Pasco G, Soufer R, Brayne C, et al. Quantitative Checklist for Autism in Toddlers (Q-CHAT). A population screening study with follow-up: the case for multiple time-point screening for autism. BMJ Paediatrics Open. 2021;5:e000700.
114. Goh DA, Gan D, Kung J, Baron-Cohen S, Allison C, Chen H, et al. Child, maternal and demographic factors influencing caregiver-reported autistic trait symptomatology in toddlers. J Autism Dev Disord. 2018;48:1325–37.
115. Hannigan LJ, Eilertsen EM, Gjerde LC, Reichborn-Kjennerud T, Eley TC, Rijsdijk FV, et al. Maternal prenatal depressive symptoms and risk for early-life psychopathology in offspring: genetic analyses in the Norwegian Mother and Child Birth Cohort Study. Lancet Psychiatry. 2018;5:808–15.

116. O'Muircheartaigh J, Robinson EC, Pietsch M, Wolfers T, Aljabar P, Grande LC, et al. Modelling brain development to detect white matter injury in term and preterm born neonates. Brain. 2020;143:467–79.
117. Marek S, Tervo-Clemmens B, Calabro FJ, Montez DF, Kay BP, Hatoum AS, et al. Reproducible brain-wide association studies require thousands of individuals. Nature. 2020;603:1–7.

ACKNOWLEDGEMENTS

We would like to acknowledge the contributions of our participants and their families; without whom, this work would not have been possible. We thank the nurses and midwives involved in data collection and the wider dHCP team.

AUTHOR CONTRIBUTIONS

The authors contributed to the article as follows: conceptualisation (AL, SV, SJC, MCC, ADE, AB), funding acquisition (ADE), data collection (AC, SF, AL), data curation and analysis (AL, AB, MP, DB, LCG, JDT, DC, JVH), supervision and project administration (AB, SV, MCC, ADE, SJC, CN, JDT, JVH), writing original draft (AL, AB), review and editing (AL, AB, MP, DB, CN, SV, MCC, ADE, SJC, LCG, JDT, DC, JVH, AC, SF). All authors approved the final version of the article prior to submission.

FUNDING

This work received funding from the European Research Council under the European Union's Seventh Framework Programme (FP7/20072013/ECR grant agreement no [319456] dHCP project) and the Medical Research Council [grant numbers MR/N013700; MR/V002465/1]. This paper represents independent research partly funded by the National Institute for Health Research (NIHR) Biomedical Research Centres at South London and Maudsley NHS Foundation Trust and at MRC Centre for Neurodevelopmental Disorders, King's College London. This work was supported by core funding from the Wellcome/EPSRC Centre for Medical Engineering [WT203148/Z/16/Z]. DC is supported by a post-doctoral fellowship of the Flemish Research Foundation (FWO) [12ZV420N]. DB received support from a Wellcome Trust Seed Award in Science [217316/Z/19/Z]. The views expressed are those of the author(s) and not necessarily those of the MRC, the NHS, the NIHR or the Department of Health and Social Care. The funders had no involvement in the collection, analysis, or interpretation of data, in the writing of the report, or in the decision to submit the article for publication.

COMPETING INTERESTS

The authors declare no competing interests.

ADDITIONAL INFORMATION

Supplementary information The online version contains supplementary material available at https://doi.org/10.1038/s41398-022-02073-y.

Correspondence and requests for materials should be addressed to Alexandra Lautarescu.

Reprints and permission information is available at http://www.nature.com/reprints

Publisher's note Springer Nature remains neutral with regard to jurisdictional claims in published maps and institutional affiliations.